Lawrence Berkeley National Laboratory

Title
Coherent Radiation in an Undulator

Permalink
https://escholarship.org/uc/item/23v6t4ds

Author
Chin, Y.H.

Publication Date
1990-12-01

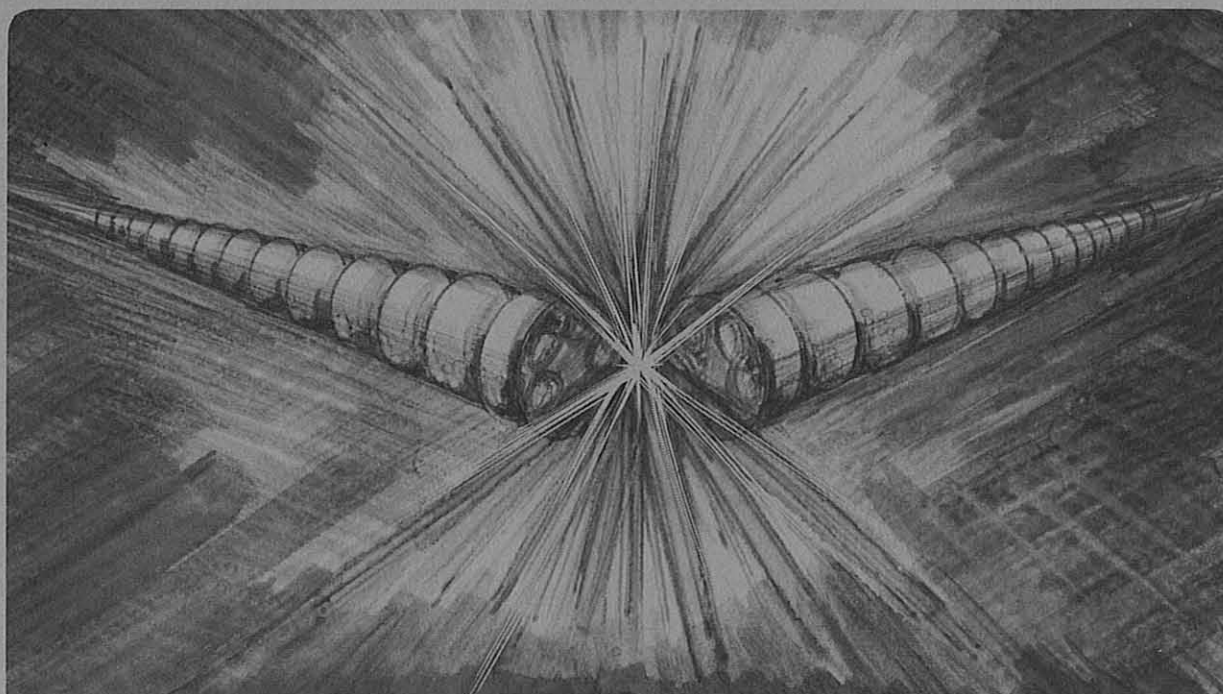# Lawrence Berkeley Laboratory
UNIVERSITY OF CALIFORNIA

Accelerator & Fusion Research Division

Presented at the Fourth Advanced ICFA Beam
Dynamics Workshop on Collective Effects in
Short Bunches BD90, Tsukuba, Japan,
September 24–29, 1990, and to be
published in the Proceedings

Coherent Radiation in an Undulator

Y.H. Chin

December 1990

DISCLAIMER

Coherent Radiation in an Undulator

Yong Ho Chin
Lawrence Berkeley Laboratory
University of California
Berkeley, CA 94720

To be Published in the Proceedings

Coherent Radiation in an Undulator*

Yong Ho Chin

Exploratory Studies Group
Accelerator & Fusion Research Division
Lawrence Berkeley Laboratory, Berkeley, CA 94720

Abstract

This paper is concerned with the synchrotron radiation from an undulating electron beam in a rectangular waveguide. The analysis is based on the dyadic Green's function approach to solve Maxwell's equations in terms of the vector potential. It is shown analytically and numerically that the radiated energy spectrum may differ significantly from the free space result when the undulator length divided by the Lorentz factor of the electron beam is larger than the transverse size of the waveguide. Then, the appearance of the spectrum is changed into a small number of sharp peaks, each corresponding to an excited waveguide mode. The undulator radiation is identified with the wake field in beam instabilities. The concepts of wake function and impedance are introduced to formulate the present problem in the same manner as the beam instability problem, so that the accumulated techniques of the latter can be applied. It is shown that the obtained impedances satisfy the Panofsky-Wenzel theorem and other properties inevitable for wake fields.

Introduction

An (plane) undulator is a device to produce high-flux quasi-monochromatic radiation in a narrow angular cone in the forward direction. A relativistic charged particle travelling in the undulator undergoes transverse oscillations and emits multipole radiation. Interference effects between the radiation fields from different poles compress the spectrum to sharp peaks. Most works on the undulator refer to radiation in free space. In reality, however, undulators are surrounded by metallic boundaries, such as a vacuum chamber. Then, the first question arises:

(1) How will the properties of the undulator radiation be changed when the boundaries are taken into account?

The radiation fields in the waveguide are modified when they reach the boundaries because they must satisfy the boundary conditions. When their wave properties match those of waveguide modes, they can survive and propagate in the waveguide. The radiated energy is redistributed among such waveguide modes. In consequence, the energy spectrum tends to change from a monotonously increasing function to discrete sharp peaks, each corresponding to an excited waveguide mode. This change is particularly of interest in the low frequency region, where the waveguide modes are

well separated. The redistribution of the radiated energy into these few modes will enhance their power significantly. If the wavelength of a waveguide mode is larger than the bunch size, the whole bunch is reinforced to move collectively by the waveguide fields. This may cause a new type of collective instability.

So far, only a few studies have been done on the influence of metallic boundaries on the radiation.[1,2] Motz and Nakamura[1] gave the first discussion on the subject by means of the Herzt vector approach to solve Maxwell's equations for an infinitely long undulator. In this paper, we present a general method to calculate the radiation fields from an undulator with finite length in the presence of a rectangular waveguide. The method is actually a generalization of Motz-Nakamura's Hertz vector method.

Once the radiation fields are calculated, the next question arises:

(2) How will the radiation fields disturb the motion of particles in a beam?

In this question, both the high and the low frequency parts of the radiation play important roles. The high frequency part will contribute to the bunching of particles on a microscopic scale, which induces coherent radiation from particles in the same bunch. This is the stimulated emission process in FEL's. The low frequency part, if it contains significant energy, will drive collective motion of the whole bunch. In both cases, the particles and the radiation fields create a coupled system. Our ultimate purpose is to solve this particle-radiation system in a self-consistent way. To this end, it is necessary first to formulate the action of the undulator radiation fields on particles. We have a similar situation in beam instability problems.[3] A charged particle interacts with its environment to create a wake field. This field acts back on the beam and disturbs the particle motion. This particle-environment system may be identified with the present particle-radiation system. With this in mind, we introduce the concepts of wake functions and their Fourier transforms, impedances.

Vector Potential

Any solutions of Maxwell's equations may be expressed in terms of the scalar potential Φ and the vector potential $\mathbf{A}$. Under the Lorentz condition, Maxwell's equations are equivalent to the two inhomogeneous wave equations for Φ and $\mathbf{A}$:

$$\nabla^2 \Phi - \frac{1}{c^2} \frac{\partial^2 \Phi}{\partial t^2} = -\frac{\rho}{\epsilon}, \tag{1}$$

$$\nabla^2 \mathbf{A} - \frac{1}{c^2} \frac{\partial^2 \mathbf{A}}{\partial t^2} = -\mu \mathbf{J}, \tag{2}$$

where c is the speed of light, ρ is the charge density, $\mathbf{J}$ is the convective current density, ϵ is the dielectric constant, and μ is the permeability. Since the scalar potential Φ can be calculated from $\mathbf{A}$ using the Lorentz condition, our task is to seek a solution for the vector potential only. To solve Eq. (2), it is useful to find a Green's function $\mathbf{G}$ which is defined as a solution of the following equation with appropriate boundary conditions:

$$\partial^2 \mathbf{G}(\mathbf{r}, t | \mathbf{r}', t') - \frac{1}{c^2} \frac{\partial^2 \mathbf{G}}{\partial t^2} = -\mathbf{I} \delta(\mathbf{r} - \mathbf{r}') \delta(t - t'), \tag{3}$$

where **G** is a 3×3 matrix, the so-called dyadic Green's function,[4] and **I** is the unit dyadic. A solution of Eq. (2) is calculated from

$$\mathbf{A}(\mathbf{r}, t) = \mu \int \int \mathbf{G}(\mathbf{r}, t | \mathbf{r}', t') \mathbf{J}(\mathbf{r}', t') d^3 \mathbf{r}' dt'. \tag{4}$$

In rectangular coordinates x, y and z, the solution **G** of Eq. (3) has only diagonal terms. The geometry of concern may be that part of a considerably longer waveguide that is sandwiched by the undulator of finite length. We assume that the walls have infinite conductivity. We denote the inside region of the waveguide by $0 \le x \le a$ and $0 \le y \le b$. Then the solution is written as [4]

$$\mathbf{G}(\mathbf{r}, t | \mathbf{r}', t') = \frac{1}{4\pi^2} \sum_{m,n \ge 0} \sum_{\nu = x,y,z} \mathbf{i}_\nu \mathbf{i}_\nu \int_{-\infty}^{\infty} d\omega \int_{-\infty}^{\infty} d\beta \frac{\phi_{mn\nu}(\mathbf{r}_\perp) \phi_{mn\nu}(\mathbf{r}'_\perp)}{\beta^2 - \omega^2/c^2 + \alpha_{mn}^2} e^{-i\beta(z-z')} e^{i\omega(t-t')},$$

$$\tag{5}$$

where

$$\alpha_{mn}^2 = (\frac{m\pi}{a})^2 + (\frac{n\pi}{b})^2. \tag{6}$$

Here $\mathbf{i}_\nu (\nu = x, y, z)$ is the unit vector, $\mathbf{r}_\perp$ is the transverse component of $\mathbf{r}$, and $\mathbf{i}_\nu \mathbf{i}_\nu$ is an operator such that $(\mathbf{i}_\nu \mathbf{i}_\nu) \cdot \mathbf{a} = (\mathbf{i}_\nu \cdot \mathbf{a}) \mathbf{i}_\nu$ for any vector $\mathbf{a}$. The functions $\phi_{mn\nu}(\mathbf{r}_\perp)$ are the eigenfunctions of waveguide modes with real eigenvalues.[4]

The integration over β in Eq. (5) can be done readily using the residue theorem. The result is

$$\mathbf{G}(\mathbf{r}, t | \mathbf{r}', t') = -\frac{i}{2\pi} \sum_{m,n,\nu} \mathbf{i}_\nu \mathbf{i}_\nu \int_{-\infty}^{\infty} d\omega \frac{\phi_{mn\nu}(\mathbf{r}_\perp) \phi_{mn\nu}(\mathbf{r}'_\perp)}{2\beta_{mn}} e^{i\omega(t-t')} e^{-i\beta_{mn}|z-z'|}, \tag{7}$$

where

$$\beta_{mn} = \frac{\omega}{c} \sqrt{1 - (\frac{c}{\omega})^2 \alpha_{mn}^2}. \tag{8}$$

Let us consider a single electron moving in the $x - z$ plane. It enters the undulator at $x = x_0, y = y_0, z = z_0$ at time $t = 0$. The undulator has length L. We assume that the particle's motion is described by

$$x = \frac{c\kappa}{\gamma\omega_0} \sin \omega_0 t + x_0, \tag{9}$$

$$y = y_0, \tag{10}$$

$$z = vt + z_0, \tag{11}$$

where $\kappa = \frac{eB}{mck_0}$, B is the undulator field, $\omega_0 (= \frac{k_0}{v})$ is the undulator frequency, γ is the Lorentz factor of the electron, m is the electron rest mass, and v is the initial longitudinal velocity of the electron. In Eqs. (9)-(11), we have kept only the lowest order terms in powers of κ/γ, assuming $\kappa/\gamma \ll 1$ (weak field approximation). The longitudinal velocity modulation term of second order in $\frac{\kappa}{\gamma}$ is neglected in the RHS of Eq. (11). It contributes mainly to higher order harmonics.

If we insert Eq. (7) and the current densities corresponding to the undulating motion, Eqs. (9)-(11), into Eq. (4) and carry out the integration over volume $\mathbf{r}'_\perp$ and time t' ($0 \le t' \le L/v$), we have for $\mathbf{A}(\mathbf{r}, t)$

$$\mathbf{A}(\mathbf{r}, t) = \frac{1}{2\pi v} \sum_{m,n,\nu} \sum_{-\infty \le p \le \infty} \mathbf{i}_\nu \phi_{mn\nu}(\mathbf{r}_\perp) I_{mnp\nu} \int_{-\infty}^{\infty} d\omega \frac{(e^{-i(\beta_p - \beta_{mn})L} - 1)}{2\epsilon \beta_{mn}(\beta_p - \beta_{mn})} e^{i\omega t - i\beta_{mn}(z - z_0)},$$

$$\tag{12}$$

3

where

$$\beta_p = \frac{\omega - p\omega_0}{v}, \quad ; p = \text{integer} \tag{13}$$

and the explicit forms of $I_{mnp\nu}$ are given by

$$I_{mnpx} = e\omega_0 \frac{ip}{\frac{m\pi}{a}} F_{mnp}, \tag{14}$$

$$I_{mnpy} = 0, \tag{15}$$

$$I_{mnpz} = evF_{mnp}, \tag{16}$$

where

$$F_{mnp} = -\frac{i}{\sqrt{ab}} \{e^{i\frac{m\pi}{a}x_0} - (-1)^p e^{-i\frac{m\pi}{a}x_0}\} J_p\left(\frac{m\pi}{a}\frac{c\kappa}{\gamma\omega_0}\right) \sin\left(\frac{n\pi}{b}y_0\right), \tag{17}$$

and $J_p(x)$ is a Bessel function. The harmonic number p emerges due to the expansion of $\begin{pmatrix} \sin \\ \cos \end{pmatrix} [\frac{m\pi}{a}(\frac{c\kappa}{\gamma\omega_0}\sin\omega_0 t + x_0)]$ by the Fourier series about $\omega_0 t$. In obtaining Eq. (12), we have neglected the contribution from the backward radiation in the laboratory frame, i.e., the $z < z'$ case. This radiation covers only the tiny part of the Doppler down-shifted frequency range between $p\omega_0/2$ and $p\omega_0$.

Radiated Energy

The power flow P along the waveguide is given by integrating the Poynting vector over the waveguide cross section at the exit:

$$P(t) = \int_0^a \int_0^b (\mathbf{E} \times \mathbf{H}) \cdot \mathbf{i}_z dx dy, \tag{18}$$

where $\mathbf{E}$ and $\mathbf{B}$ are the electromagnetic fields calculated from the vector potential $\mathbf{A}(\mathbf{r}, t)$ given by Eq. (12) with x_0 and y_0 set to the values at the center of the waveguide. The total radiated energy U is the time integral of $P(t)$:

$$U = \int_{-\infty}^{\infty} P(t) dt. \tag{19}$$

This can be expressed by the Fourier transforms $\tilde{\mathbf{E}}(\omega)$ and $\tilde{\mathbf{H}}(\omega)$ of $\mathbf{E}(t)$ and $\mathbf{H}(t)$, respectively, as

$$U = 2\pi \int_0^a \int_0^b \int_{-\infty}^{\infty} (\tilde{\mathbf{E}}(\omega) \times \tilde{\mathbf{H}}^*(\omega)) \cdot \mathbf{i}_z d\omega dx dy. \tag{20}$$

After tedious calculation, we have

$$U = \sum_{m,n\geq 0} \sum_{-\infty \leq p \leq \infty} A_{mnp}^{(E)} \int_{-\infty}^{\infty} Z_{mnp}^{(E)}(\omega) d\omega, \tag{21}$$

where

$$\begin{aligned} A_{mnp}^{(E)} &= \frac{e^2}{2\pi} L^2 |F_{mnp}(x_0 = \frac{a}{2}, y_0 = \frac{b}{2})|^2 \\ &= \frac{4e^2}{2\pi} \frac{L^2}{ab} \sin^2\left(\frac{n\pi}{b}\right) J_p^2\left(\frac{m\pi}{a}\frac{c\kappa}{\gamma\omega_0}\right) \times \begin{cases} \cos^2\left(\frac{m\pi}{a}\right) & \text{for } p = \text{odd} \\ \sin^2\left(\frac{m\pi}{a}\right) & \text{for } p = \text{even} \end{cases} \end{aligned} \tag{22}$$

4

$$Z_{mnp}^{(E)}(\omega) = \frac{1}{4\epsilon\omega\beta_{mn}}[(\frac{\omega}{c})^2(1+(\frac{p\omega_0}{v})^2(\frac{a}{m\pi})^2) - (\beta_{mn}+\frac{p\omega_0}{v})^2]\frac{\sin^2(\beta_p-\beta_{mn})L/2}{((\beta_p-\beta_{mn})L/2)^2}, \quad (23)$$

where we have neglected the cross terms between different harmonics p. They drop out if the undulator is sufficiently long. The quantity $A_{mnp}^{(E)}$ depends on the particle orbit and provides the selection rule about mode number: n =odd, $m+p$ =odd. On the other hand, the quantity $Z_{mnp}^{(E)}(\omega)$ has the dimensions of impedance, and indeed can be identified as an impedance, as will be confirmed later. The product $A_{mnp}^{(E)}Z_{mnp}^{(E)}(\omega)$ represents the energy flow of the radiation of the p-th harmonic from the undulating electron into the waveguide mode specified by (m,n). Note that $Z_{mnp}^{(E)}(\omega)$ is always positive and is an even function of ω, being accompanied with a change in sign of p.

Now let us take a close look at $Z_{mnp}^{(E)}(\omega)$. The sink function $\frac{\sin^2(\beta_p-\beta_{mn})L/2}{((\beta_p-\beta_{mn})L/2)^2}$ represents phase matching condition. The straight line $\beta = \beta_p = \frac{\omega-p\omega_0}{v}$ expresses the resonance condition between the particle and the radiation field of the p-th harmonic. The curved line $\beta = \beta_{mn} = \frac{\omega}{c}\sqrt{1-(\frac{c}{\omega})^2\alpha_{mn}^2}$ or $\beta^2 = (\frac{\omega}{c})^2 - \alpha_{mn}^2$ represents the dispersion relation of the structure for the waveguide mode (m,n). The factor $\frac{\sin^2(\beta_p-\beta_{mn})L/2}{((\beta_p-\beta_{mn})L/2)^2}$ is peaked at the frequencies where the two lines cross. The two intersections correspond to the excited waveguide modes which move together with the electron having the same speed, so that they can interact over a prolonged period of time. The peak frequencies are obtained by solving $\beta_p = \beta_{mn}$ for ω. The result is

$$\omega = \omega_\pm = \gamma^2[p\omega_0 \pm \frac{v}{c}\sqrt{(p\omega_0)^2 - \frac{c^2}{\gamma^2}\alpha_{mn}^2}]. \quad (24)$$

The signs $+$ and $-$ correspond to the Doppler up- and down-shifted frequencies of the radiation fields emitted in the forward and the backward directions, respectively, in the electron rest frame.

Figure 1 shows an example of the energy spectrum. The parameters used, $\gamma = 5.9$, $\lambda_0 =$ the undulator wavelength $= 2.77$ cm, $a = 13.34$ cm, $b = 1.9$ cm, and $N = L/\lambda_0 = 258$, are relevant to those of the University of California at Santa Barbara (UCSB) FEL. The peak frequency corresponds to the wavelength of 0.4 mm. The free space spectrum denoted by the broken line is drawn for comparison. One can recognize that the interference effects due to the boundary change the spectrum significantly from the free space result.

A criterion for the transverse size of the waveguide for which the boundary effects may be neglected (we assume always $a \geq b$)

$$b \geq L/\gamma \quad (25)$$

can be derived from the following physical consideration. In the electron rest frame, the length of the undulator is L/γ. If the radiation emitted at the entrance of the undulator cannot, after bouncing at the boundary, come back to the electron by the time when the electron gets out of the undulator, the electron cannot know the existence of the boundary. In other words, since the information about the boundary does not reach the electron, the boundary effects cannot influence the interaction properties between the electron and the radiation fields. The fastest information may be brought back by the fields radiated into the purely vertical direction. It takes time b/c. This value has to be larger than $L/(\gamma c)$.
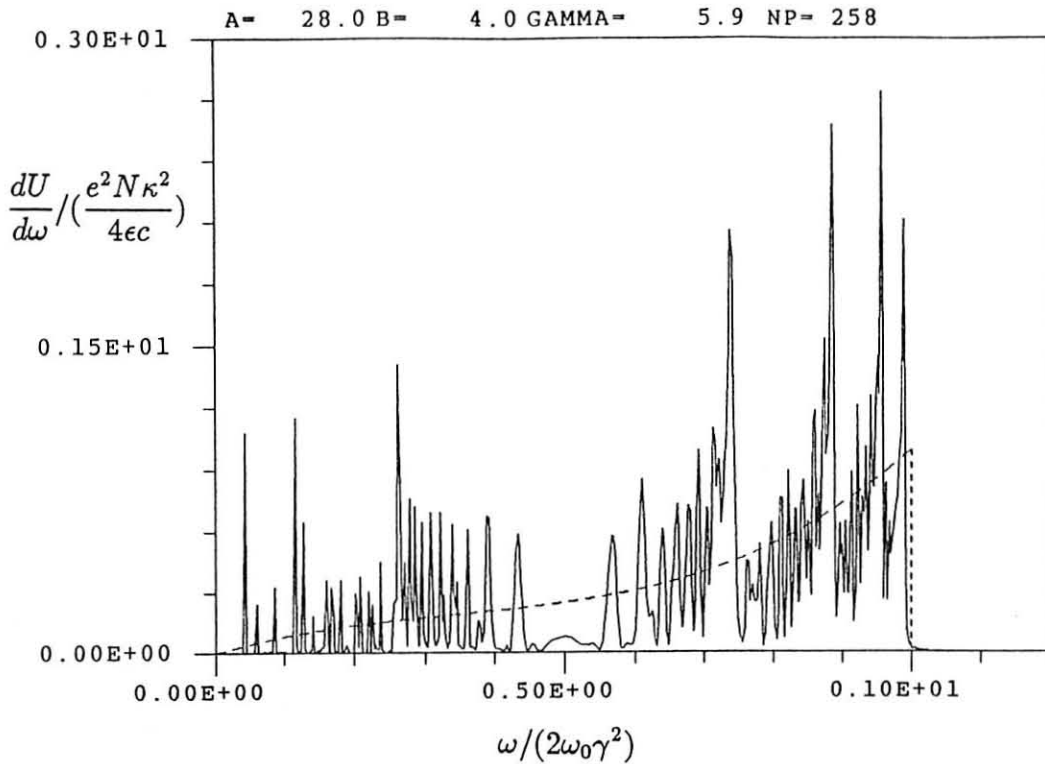
5

Figure 1: Radiated energy spectrum of UCSB FEL. The free space result is denoted by the broken line.

Wake Function and Impedance

We here would like to study the action of the radiation on particles in a beam. If we are allowed to neglect the perturbation in particle motions due to the radiation fields while particles go through the undulator, we can apply the concepts of wake function and its Fourier transform, impedance.[3] Suppose a charged particle travelling through an undulator, emitting the radiation. We call it the driving particle. Imagine another particle (test particle) which moves together with the driving particle keeping the fixed distance $Z = Tv$. The wake function is defined by the total Lorenzt force exerted on the test particle over the structure from the radiation fields. The test particle may go either ahead of or behind the driving particle. This is the peculiar point of the present problem different from the beam instability case where we consider only the test particle following the driving particle since there is no fields ahead of the driving particle. The wake function contains the longitudinal and the transverse components. They may be written explicitly as

$$W_x(T) = \int d^3\mathbf{r} \int_T^{T+\frac{L}{v}} dt \rho \cdot (E_x - v_z B_y), \tag{26}$$

$$W_y(T) = \int d^3\mathbf{r} \int_T^{T+\frac{L}{v}} dt \rho \cdot (E_y + v_z B_x - v_x B_z), \tag{27}$$

$$W_z(T) = -\int d^3\mathbf{r} \int_T^{T+\frac{L}{v}} dt \rho \cdot (E_z + v_x B_y), \tag{28}$$

6

where ρ is the charge density of the test particle. Note the minus sign in the definition of the longitudinal wake function. This follows the convention of the beam instability formalism where $W_z(T)$ is always negative, i.e., the test particle is decelerated, in the vicinity of the driving particle. If the test particle is the same particle as the driving one ($T = 0$), the longitudinal wake function gives the energy loss of the particle due to deceleration by its own fields. This energy loss is nothing but the total radiated energy, namely,

$$W_z(0) = U. \tag{29}$$

The wake function generalizes the concept of the radiated energy to the case where the particle that creates the radiation fields and the particle that feels them are different.

Carrying out the integration in Eqs. (26)-(28), we obtain,

$$W_\nu(T) = \sum_{m,n \geq 0} \sum_{-\infty \leq p \leq \infty} A_{mnp\nu} W_{mnp\nu}(T) \tag{30}$$

with

$$W_{mnp\nu}(T) = \begin{cases} \dfrac{1}{i}\displaystyle\int_{-\infty}^{\infty} Z_{mnp\nu}(\omega)e^{i\omega T}d\omega & \text{for } \nu = x \text{ or } y \\ \displaystyle\int_{-\infty}^{\infty} Z_{mnp\nu}(\omega)e^{i\omega T}d\omega & \text{for } \nu = z \end{cases} \tag{31}$$

where

$$Z_{mnpx}(\omega) = \frac{\frac{m\pi}{a}}{2\epsilon\omega\beta_{mn}}\{(\frac{a}{m\pi})^2\frac{\omega}{v}\frac{p\omega_0}{c}(\frac{\omega}{c} - \frac{v}{c}\beta_{mn}) - (\beta_{mn} + \frac{p\omega_0}{v}) + \frac{v^2}{c^2}\frac{\omega}{v}\}$$
$$\times \frac{\sin^2(\beta_p - \beta_{mn})L/2}{((\beta_p - \beta_{mn})L/2)^2}, \tag{32}$$

$$Z_{mnpy}(\omega) = \frac{\frac{n\pi}{b}}{2\epsilon\omega\beta_{mn}}\{(\frac{a}{m\pi})^2\frac{\omega}{v}(\frac{p\omega_0}{c})^2 - (\beta_{mn} + \frac{p\omega_0}{v}) + \frac{v^2}{c^2}\frac{\omega}{v}\}\frac{\sin^2(\beta_p - \beta_{mn})L/2}{((\beta_p - \beta_{mn})L/2)^2}, \tag{33}$$

$$Z_{mnpz}(\omega) = \frac{\frac{\omega}{v}}{2\epsilon\omega\beta_{mn}}\{(\frac{a}{m\pi})^2\beta_{mn}(\frac{p\omega_0}{c})^2 - \frac{1}{\gamma^2}\frac{\omega - p\omega_0}{v}\}\frac{\sin^2(\beta_p - \beta_{mn})L/2}{((\beta_p - \beta_{mn})L/2)^2}, \tag{34}$$

and we have neglected the cross terms between different harmonics p. As in the previous section, we call $Z_{mnp\nu}(\omega)$ the impedance. The explicit forms of $A_{mnp\nu}$ are as follows:

$$A_{mnpx} = \begin{cases} \dfrac{e^2}{2\pi}\dfrac{4L^2}{ab}\cos(\frac{m\pi}{a}x_0)\sin(\frac{m\pi}{a}x_1)\sin(\frac{n\pi}{b}y_0)\sin(\frac{n\pi}{b}y_1)\mathrm{J}_p^2(\frac{m\pi}{a}\frac{c\kappa}{\gamma\omega_0}) & \text{for } p = \text{odd} \\ \dfrac{e^2}{2\pi}\dfrac{4L^2}{ab}\sin(\frac{m\pi}{a}x_0)\cos(\frac{m\pi}{a}x_1)\sin(\frac{n\pi}{b}y_0)\sin(\frac{n\pi}{b}y_1)\mathrm{J}_p^2(\frac{m\pi}{a}\frac{c\kappa}{\gamma\omega_0}) & \text{for } p = \text{even,} \end{cases} \tag{35}$$

$$A_{mnpy} = \begin{cases} \dfrac{e^2}{2\pi}\dfrac{4L^2}{ab}\cos(\frac{m\pi}{a}x_0)\cos(\frac{m\pi}{a}x_1)\sin(\frac{n\pi}{b}y_0)\cos(\frac{n\pi}{b}y_1)\mathrm{J}_p^2(\frac{m\pi}{a}\frac{c\kappa}{\gamma\omega_0}) & \text{for } p = \text{odd} \\ \dfrac{e^2}{2\pi}\dfrac{4L^2}{ab}\sin(\frac{m\pi}{a}x_0)\sin(\frac{m\pi}{a}x_1)\sin(\frac{n\pi}{b}y_0)\cos(\frac{n\pi}{b}y_1)\mathrm{J}_p^2(\frac{m\pi}{a}\frac{c\kappa}{\gamma\omega_0}) & \text{for } p = \text{even,} \end{cases} \tag{36}$$

$$A_{mnpz} = \begin{cases} \dfrac{e^2}{2\pi}\dfrac{4L^2}{ab}\cos(\frac{m\pi}{a}x_0)\cos(\frac{m\pi}{a}x_1)\sin(\frac{n\pi}{b}y_0)\sin(\frac{n\pi}{b}y_1)\mathrm{J}_p^2(\frac{m\pi}{a}\frac{c\kappa}{\gamma\omega_0}) & \text{for } p = \text{odd} \\ \dfrac{e^2}{2\pi}\dfrac{4L^2}{ab}\sin(\frac{m\pi}{a}x_0)\sin(\frac{m\pi}{a}x_1)\sin(\frac{n\pi}{b}y_0)\sin(\frac{n\pi}{b}y_1)\mathrm{J}_p^2(\frac{m\pi}{a}\frac{c\kappa}{\gamma\omega_0}) & \text{for } p = \text{even.} \end{cases} \tag{37}$$

Some conclusions may be drawn from inspection of Eqs. (30) to (37).

(1) The transverse impedances are odd functions of frequency ω in connection with the change in sign of p:

$$Z_{mnp\nu}(\omega) = -Z_{mn,-p\nu}(-\omega) \geq 0 \quad \text{for } \nu = x \text{ or } y, \tag{38}$$

while the longitudinal impedance is an even function of ω:

$$Z_{mnpz}(\omega) = Z_{mn,-pz}(-\omega) \geq 0. \tag{39}$$

This implies that

$$W_{mnp\nu}(0) = 0 \quad \text{for } \nu = x \text{ or } y \tag{40}$$

which means that a particle receives no net transverse force from its own radiation.

(2) If we take the limit of infinitely long waveguide, i.e., $L \to \infty$, we find that the following relationships hold between the transverse and the longitudinal impedances for the same set of (m, n, p)

$$Z_{mnpz}(\omega) = \frac{\omega - p\omega_0}{v}\left(\frac{a}{m\pi}\right)Z_{mnpx}(\omega), \tag{41}$$

$$Z_{mnpz}(\omega) = \frac{\omega - p\omega_0}{v}\left(\frac{b}{n\pi}\right)Z_{mnpy}(\omega). \tag{42}$$

The above relationships are quite similar to the Panofsky-Wenzel theorem [3] except for the factor $(\omega - p\omega_0)/v$ instead of ω/v. The appearance of $\frac{p\omega_0}{v}$ might originate from the characteristics of the undulating orbit of the particle.

(3) From Eqs. (35)-(37) and (30), we notice that

$$W_x(T) = 0 \quad \text{if } x_0 = x_1 = \frac{a}{2}, \tag{43}$$

$$W_y(T) = 0 \quad \text{if } y_0 = y_1 = \frac{b}{2}. \tag{44}$$

This is obvious from the geometrical symmetry of the particle trajectory and the wave guide.

In carrying out the integration in Eq. (31), it is necessary to separate the frequency range of the integration in impedance according to the sign of T. Namely, the test particle lagging behind or going ahead of the driving particle sees a different frequency range of the impedance. There is the following physical reason for this case distinction. For simplicity, let us consider the radiation in free space. In the electron rest frame, Power flow to the radiation must be the same in the forward and backward directions for symmetry. Most of the backward radiation in the electron rest frame is turned around into the forward direction in the laboratory frame by the Lorentz transformation. The plane $z' = 0$ perpendicular to the z'-axis in the electron rest frame now forms a narrow cone about the z-axis with the angle $\theta = 1/\gamma$. This cone sets the border that separates the two kinds of the forward radiation having different origins. The radiation inside and outside of the cone correspond to the forward and the backward radiations in the electron rest frame, respectively. The test particle lagging behind the driving particle in the laboratory frame is also sitting behind it in the electron rest frame. Therefore it can feel only the backward radiation in the rest frame. It sees the forward radiation

outside of the cone and the backward radiation in the laboratory frame. The test particle going ahead of the driving particle sees the forward radiation in the electron rest frame and the corresponding forward radiation inside of the cone in the laboratory frame.

The frequency of the radiation fields emitted along the cone can be easily calculated from the Lorentz transformation: that is $\omega_{cone} = p\omega_0\gamma^2$ which is just half the peak frequency $2p\omega_0\gamma^2$. The backward radiation in the laboratory frame covers only the very low frequency region from $p\omega_0/2$ to $p\omega_0$. Its total power is about γ^2 times smaller than that of the forward radiation. Thus, the backward radiation may be neglected for ultra-relativistic particles. From the above arguments, we can conclude that for $T > (<)0$, i.e, when the test particle lags behind (goes ahead of) the driving particle, the integral in Eq. (31) should be done over the frequency range from 0 ($p\omega_0\gamma^2$) to $p\omega_0\gamma^2$ (∞).

Figure 2 shows an example of the longitudinal wake function. Again, the parameters are taken from those of the UCSB FEL. One can see that the wake function is significant only in the close vicinity of the driving particle ($\Delta T \sim 2\pi/(\omega_0\gamma^2)$). This is due to the rapidly oscillating phase factor $e^{i\omega T}$ in the integrand for large T. The broken line denotes the wake function from free space radiation. Even for a small value of the transverse size, no large differences in the wake functions are recognizable, although the energy spectra are quite different (see Fig. 1). This suggests that the free space radiation result for the wake function may be used as a good approximation to any structure.

If we compare Eqs. (21)-(23) with Eqs. (30)-(37) and neglect the quantities smaller than the leading term by a factor γ^2, we can conclude that

$$\frac{1}{2}(W_z(0_+) + W_z(0_-)) = U = W_z(0). \tag{45}$$

This approximation is consistent with having ignored the longitudinal velocity modulation term in Eq. (11) and the backward radiation in the Green's function. In fact, the relationship(45) is a physical consequence of energy conservation and can be derived from the following thought experiment. Suppose that the test particle follows the driving particle at an infinitesimal distance and that they have opposite unit charges. Here the test particle is a real particle, i.e., it also emits radiation. Both particles lose energy U by radiation, while the test and the driving particles gain an energy $W_z(0_-)$ and $W_z(0_+)$, respectively, from the fields radiated by the other particle. When they are put together, the charges will be neutralized and the radiation is suppressed. In order for the total energy to be conserved, we need

$$W_z(0_+) + W_z(0_-) = 2U \tag{46}$$

which agrees with Eq. (45). The above relationship is a modified form of the fundamental theorem of beam loading.[3]

$$\frac{W_z(T)}{\frac{e^2 N \kappa^2}{4\epsilon c}\omega_0\gamma^2}$$

A= 28.0 B= 4.0 GAMMA= 5.9 NP= 258

0.12E+01

0.00E+00

-.12E+01

-.10E+02   0.00E+00   0.10E+02

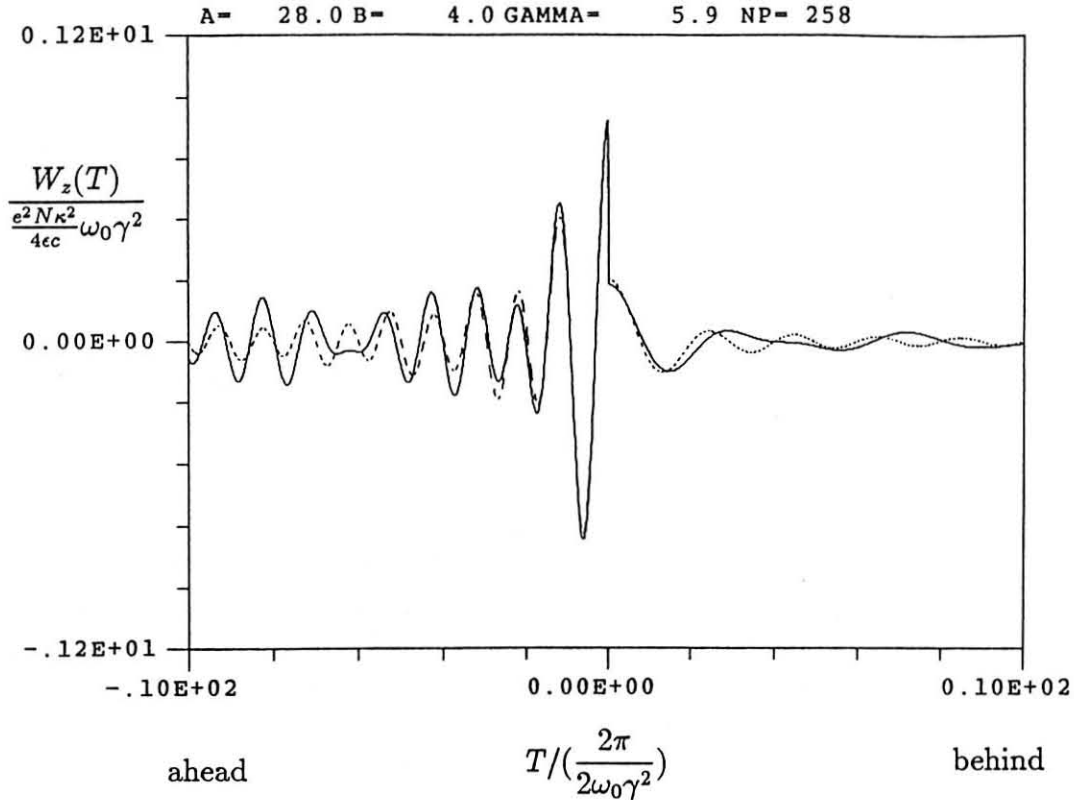ahead $T/(\frac{2\pi}{2\omega_0\gamma^2})$ behind

Figure 2: Longitudinal wake function of the UCSB FEL.

Conclusions

The identification of the undulator radiation with the wake field in beam instabilities seems to be proper. The difference is only that the wake function is significant mostly ahead of the driving particle in the case of undulator radiation, while it is non-zero only behind the driving particle in usual wake fields. The longitudinal wake function includes necessary information on how particles will be accelerated or decelerated by the radiation fields. From this, one can calculate the bunching of particles and eventually explain the stimulated emission process. In the analyses of FEL behavior so far, the bunching has been estimated by picking up only the radiation field emitted on axis in the forward direction. As a result, the wake function becomes a periodic function of the distance from the driving particle, and one needs to impose an arbitrary upper limit on the distance that the force can reach. The present analysis removes such arbitrariness. Future study will be aimed towards solving the particle-radiation system in a self-consistent way in order to clarify the coherent radiation mechanism.

References

1. H. Motz and M. Nakamura, Ann. Phys., **7**, 84(1959).
2. Y. H. Chin, in *Proc. of the 1989 IEEE Particle Accelerator Conference*, (Chicago, IL, March, 1989), pp. 809-811.
3. A. W. Chao, SLAC Report, SLAC-PUB-2946, June, 1982.
4. R. E. Collin, *Field Theory of Guided Waves* (McGraw-Hill, New York, 1960).